Probabilistic Fatigue Life Assessment of an Offshore Wind Turbine in Greece

Dimitrios V. Bilionis and Dimitrios Vamvatsikos
School of Civil Engineering, National Technical University of Athens.
Zografou, Athens, Greece

ABSTRACT

Wind Turbines constitute a sustainable and effective solution for the production of energy using wind power. Offshore wind turbines especially are becoming of special interest. The purpose of this paper is to provide a case study of fatigue life assessment for specific cross-sections of a standard offshore wind turbine with a monopile design, under a probabilistic framework. Two potential sites of construction in the Aegean Sea of Greece were examined. The results show the dependence of fatigue life on the local wind and wave conditions, the cross-section geometry and the welded connection detailing. All in all, the more benign conditions in the Aegean allow simpler connection details to still have acceptable performance.

KEY WORDS: Offshore Wind Turbine; Monopile Design; Fatigue; Aegean Sea

INTRODUCTION

Wind turbines constitute a sustainable and effective solution for the production of energy using wind power. Wind turbines may be constructed either in land areas (onshore) or in sea areas (offshore). Offshore wind turbines are becoming of special interest in recent years. Although an offshore wind turbine usually starts with a higher initial cost, it can outweigh a similar onshore one during its service life regarding a number of aspects such as: higher productivity due to stronger winds over sea areas, larger available installation areas and lower (or even non-existent) public nuisance. The latter is especially important in countries such as Greece where protracted court battles have hindered most onshore wind farms, inflicting substantial cost and crippling delays.

A wind turbine could be considered as a structure that lies between a civil engineering structure and a machine (Sorensen, 2014). In specific, a wind turbine consists of structural elements (tower, substructure etc.) and a number of electrical and machine components with a control system (gear box, drivetrain etc.). Under a civil engineering perspective, the main components of a wind turbine could be considered the tower and the substructure system. The tower is the element on the top of which the mechanical parts of the wind turbine, such as the nacelle and the blades, are installed. The tower is made of steel and has a circular cross-section. It is usually tapered i.e. the cross-section size (e.g. diameter, thickness etc.) decreases with height, typically in a linear fashion. The tower is connected to the substructure, i.e., the part of the wind turbine that is submerged in the water. The substructure may be founded directly in the seabed or based on a floating platform. This type of the substructure's foundation usually distinguishes an offshore wind turbine into two categories, namely fixed and floating. Fixed wind turbines are used especially in sites of low or medium depths, while the construction of a floating wind turbine is cost-effective in the case of deep waters. The most common type of design for fixed wind turbines, which is used for depths up to 30 meters, is the monopile. This is probably the simplest structural concept, where the tower is connected (directly or via a transition piece) to a pile that has been founded at the seabed.

Regardless of the type of an offshore wind turbine, both structure and substructure are subject to dynamic combinations of wind and wave loads with a wide range of frequencies. This fact may raise critical issues during the turbine's service life in terms of fatigue and power efficiency (Jonkman, 2009). For this reason, special focus should be devoted on the appropriate analysis and assessment of the dynamic combination of loads during the design phase. Furthermore, since wind turbines are complicated structures including a number of different components, reliability analysis considering consistent reliability levels and taking into account the dynamic nature of loads has received considerable attention by researchers (Sorensen 2014; Moan 2014). However, a great challenge in the above analysis is posed by the stochastic nature of the main loading mechanisms, namely wind and wave, as their characteristics tend to vary rapidly. Their stochasticity mainly depends on the climate at the area of construction. Thus, one could say that the design of an offshore wind turbine is a highly site-specific process. For this reason, the use of accurate site anemological and wave data is essential.

As far as the loads are concerned, the aforementioned stochasticity affects their magnitude and also subjects the structure to cyclic stresses making its components vulnerable to fatigue damage. Furthermore, it affects the overall performance and energy output. Research efforts are currently under way to incorporate climate information and relate it directly to the calculation of fatigue damage (Passon and Branner, 2014) or the assessment of performance (Arwade et al., 2011). However the stochastic nature of the wind and waves, as physical phenomena, makes such an analysis very complicated and appropriate methods from statistics and probability theory need to be incorporated.

The purpose of this paper is to provide a case study of a probabilistic fatigue life assessment for a standard offshore wind turbine located in

the Aegean Sea of Greece. In specific, a fixed offshore wind turbine with a monopile foundation is studied. Two potential sites of construction, one in the north part and another in the south part of Aegean, with different wind and wave characteristics, are considered. In both sites, extreme event load cases were not found to influence the design, thus our focus is on fatigue damage for different wind-wave states and for specific cross-sections of the structure. Furthermore, an estimation of the expected fatigue life is made by incorporating Monte Carlo simulation.

THE WIND TURBINE MODEL

The National Renewable Energy Laboratory (NREL) 5MW Baseline Wind Turbine was selected as a standard offshore wind turbine for this study. The rated power is 5 MW. The tower of the turbine is tapered and of steel circular hollow cross-section. The base diameter is 6.00 m and the thickness 27 mm, while the top diameter is 3.87 m with a thickness of 19 mm. The height of the tower at its top point (where the nacelle is based) is at 87.60 m from the Mean Sea Level (MSL). The rotor has three blades. The rotor disk has a diameter of 126.00 m and its center (hub height) is located at 90.00 m from the MSL. The cut-in and cut-out wind speeds are 3 m/s and 25 m/s respectively. For additional details regarding the characteristics of the standard turbine the reader may refer to Jonkman et al. (2009). The tower is connected to a monopile foundation via a transition piece (TP). The monopile is considered to be founded at a depth of 28 m. It has a steel circular hollow cross-section, 6.00 m in diameter and 60mm thick. The connection of the base of the tower to the transition piece is considered to be at 10.00 m of the MSL (Fig. 1). Finally, a rigid type of foundation is assumed at mudline.

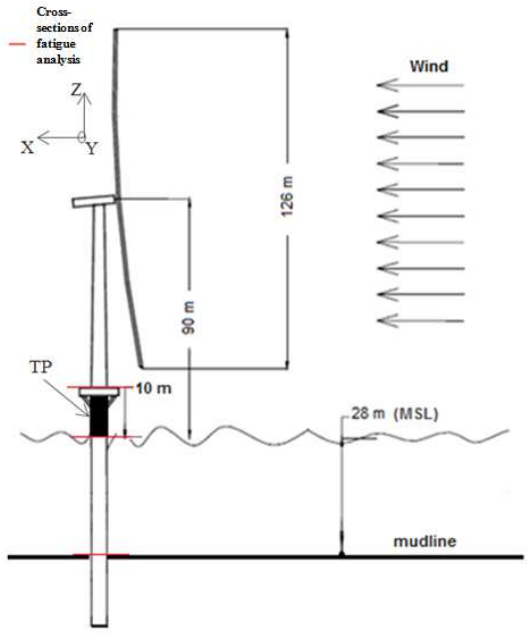

Fig. 1. Wind Turbine Model (adapted from Kooijman et al. 2003).

THEORETICAL BACKGROUND

Design criteria and analysis guidance are provided by published standards. The analysis of offshore wind turbines is mainly based on the IEC 61400-3 standard (IEC, 2009). It specifies the context for the assessment of external conditions and the design requirements to ensure the engineering integrity of the structure. The IEC standard also provides an appropriate level of protection from all hazards during the planned lifetime of an offshore wind turbine. In addition, the DNV standards (DNV, 2010) can also be used for the assessment of loads on marine structures subjected to wind, wave and current loading.

Loads

The assessment of wind loads is critical for the analysis of an offshore wind turbine. Although wind is essential for the operation and efficiency of a wind turbine, it is also the environmental factor with the greatest contribution to the loading of the structure. For the assessment of wind loads, time-series of wind speed at the hub height of the wind turbine are used. The time-series may have been developed according to specific spectrums (such as Kaimal or von Karman), based on the characteristic (average) value of a 10-minute wind speed. For this process appropriate software can be used, such as the TurbSim software developed by NREL (Jonkman and Kilcher, 2012) and adopted in this study. The wind time-series are then used as the input to calculate the values of reactions and deflections at the structure due to the wind. In this study, the FAST software was used (Jonkman and Buhl, 2005).

Offshore wind turbines are also subject to wave loads which in some cases (e.g. in North Seas) may be very significant. Wave characteristics, such as the significant wave height (H_s) and peak spectral period (T_p), depend on the wind speed and the available sea length, or fetch, over which the wind transfers energy to the sea. Several methodologies and associated wave spectra are available for the calculation of the dynamic wave characteristics. A very widely used spectrum is JONSWAP (IEC 61400-3; DNV 2010) that will also be our choice. A simplified method to transform wave characteristics into forces on a structure is the Morison equation (Morison et al., 1950). This is a semi-empirical method for calculating the acting force on a body (e.g. a pile) that is submerged into moving water. The general form of the equation is as follows:

$$F = C_M \rho A \frac{du}{dt} + C_D \frac{1}{2} \rho D |u| u \quad (1)$$

where: D is the diameter of the member (pile), C_D and C_M are the drag and inertial coefficients respectively, ρ is the water density, A is the cross-sectional area and u is the water velocity relative to the body. The forces and the moments acting on the structure are then calculated by integrating the height-wise contributions of Eq. 1. For more details about the application of the Morison equation, the reader may refer to DNV 2010.

Uncoupled vs Coupled Analysis

An important challenge in the analysis of an offshore wind turbine is the integration of the wind and wave effects that act simultaneously on the structure. In practice, two different approaches may be used, namely the uncoupled and coupled method. In uncoupled analysis the loads due to the wind are calculated independently from the loads due to the waves and finally the total loads are calculated by linear superposition. In this case the assumption is made that the tower is practically rigid. Thus it is essentially immobile, making the absolute wave velocity equal to the relative that appears in Eq.1. Similarly, the position of the rotor disk is assumed not to be influenced by the waves. Of course, this assumption may not fully correspond to the real acting mechanisms of the wind and waves on the structure. However, despite the above weakness, uncoupled analysis may be useful since it is associated with lower computational effort than a fully coupled analysis (Moan, 2014) and it allows the blending of different software to

perform the two types of analyses. Thus, commercial finite element software can be employed that can capture the details of the structure and achieve accurate stress calculations. On the other hand, in a coupled analysis the wind and waves are act simultaneously on the structure. It is clear that this method is more realistic (Moan 2014) as it properly captures the dynamic nature of the problem, at the cost of needing specialized software.

In the initial phase of this study, both types of analysis (uncoupled and coupled) were performed. In the uncoupled analysis, the wind loads were calculated using FAST, while the wave loads were calculated from Eq. 1 for wind-compatible sea-states. Fig. 2 shows comparison graphs of average values of the overturning moment at mudline, which corresponds to the reaction moment along global Y axis (top graph) and of the maximum absolute value of that moment (bottom graph) for different wind speeds at hub height as they were calculated by using a time-series of 10-minute length. As far as the maximum absolute value of the overturning moment is concerned, the values from the coupled analysis are quite higher. On the other hand, there is no practical difference in the average values. These findings echo the views of other researchers as well (e.g., Haselbach, 2013) and, although not conclusively ruling out the possibility of using uncoupled analysis, they led us to only employ coupled analyses in our investigation.

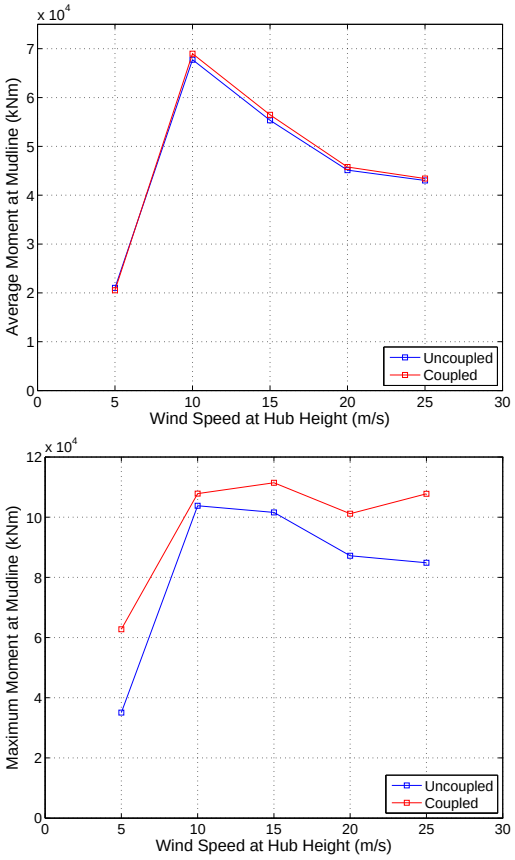

Fig. 2. Comparison of results between uncoupled and coupled analysis. Average moments (top) are similar, while maximum absolute ones (bottom) are not.

Fatigue

According to Eurocode 3 (EC3), fatigue is considered as the damage in a member of a structure through crack initiation and/or crack propagation due to repeated stress fluctuations. Various standards have been published for the design of steel structures against fatigue. In the Eurocode series, part 1.9 of EC3 (2002) provides the analysis context for fatigue design of steel structures. For the estimation of fatigue damage, time-series of stress history associated with the structural member of interest are needed. After those time-series are obtained, the stresses of various magnitudes should be grouped into groups of specific stress magnitude. Then, the number of cycles (i.e. the frequency) of each group is counted. A very widely used approach for counting the number of cycles is the rainflow counting algorithm (ASTM, 1997; Nieslony, 2009).

By incorporating rainflow counting, the number of cycles of stress is calculated for each of the different groups of stress amplitudes. Particular attention is paid to handling (or "closing") half-cycles (e.g. Hayman 2012) and adding their damage. Once the number of cycles for each group is specified, the corresponding fatigue damage can be estimated. In specific, if n_i is the number of cycles observed for stress group i, and N_{fi} is the number of cycles to failure for stress group i, the corresponding damage d_i is:

$$d_i = \frac{n_i}{N_{fi}} \tag{2}$$

The total damage D in a stress history of a specific length is then calculated by the following formula (Palmgren-Miner rule):

$$D = \sum_{i=1}^{k} d_i = \sum_{i=1}^{k} \frac{n_i}{N_{fi}} \tag{3}$$

The fatigue life of a structural member is the time until D reaches the maximum allowable value of 1. Assuming that D has been estimated for a representative enough interval of duration T_D over which its accumulation may be assumed to be stationary, a good estimate (assuming deterministic capacity) of the corresponding fatigue life is equal to T_D/D. For instance, if D is the mean annual fatigue damage of a member, the estimated fatigue life in years is equal to $1/D$.

CASE STUDIES FOR GREECE

Offshore wind farms have been constructed and are in operation in the northern seas of Europe. On the other hand, none have been installed in the Mediterranean Sea. However, a number of projects are ongoing for examining the potential of design and installation of offshore wind farms by several Mediterranean countries (MedPAN, 2013). In this paper, two case studies will be presented for the preliminary assessment of fatigue life in three different cross-sections of a standard offshore wind turbine with a monopile foundation (Fig. 1). In specific, two different sites in the Aegean Sea of Greece were selected, shown in the map of Fig. 3.

The first site is located on the North part of the Aegean, while the second site on the South part. Each has its own wind and wave characteristics, in large part due to the difference in the surrounding geography. For the case of the North site, due to the proximity of the mainland, significant difference in fetch exists for the various wind directions, with the maximum appearing for a southern wind. In the case of the South site though, no much difference could be assumed between the different directions and a practically uniform fetch could be used for the analysis.

Fig. 3. Map of Aegean Sea with the examined installation sites.

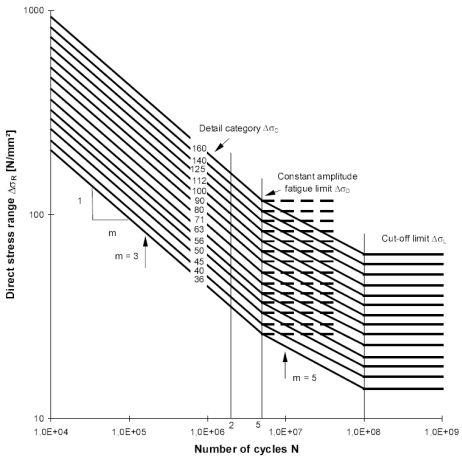

Fig. 4. S-N curves for structural steel from EC3 Part 1.9

Analysis Process

For both sites of the study a similar process was followed for the estimation of the fatigue life. First, anemological data was obtained from the National Weather Service of Greece. A statistical analysis for specifying the major trends and the distribution of that data was performed. Given the relatively small fetch distances in the Aegean, the wind speed is reasonably assumed to fully determine the wave state as well, something that would not be true, for example, in an ocean environment. Thus, the wave characteristics (significant wave height and peak period) were calculated based on the JONSWAP spectrum for each possible value of *local* wind speed. Finally, the joint probability density function (joint PDF) of wind speed (U_{10}) and significant wave height (H_s) were estimated, a process that will be discussed in more detail in the next subsection.

For the analysis of loads, time-series of wind speed at the hub height were simulated using the TurbSim software. In specific, time-series of 10-minute length were developed for a number of wind speed values, ranging from 3 m/s (cut-in) to 25 m/s (cut-out) to represent operational conditions and at 30 m/s for the parked turbine. The aforementioned time-series along with the corresponding wave characteristics constituted the input for the FAST software, where the coupled dynamic analysis of wind and wave loadings was performed.

A number of 10 simulations were performed for each mean wind speed and direction. In each case, appropriate wave data for period and height were generated according to the JONSWAP spectrum for the corresponding fetch distance at the site. At the end of each simulation, 10-minute time-series of reaction forces, moments, deflections and other values on the structure were obtained. Based on those time-series, stress histories were assessed for different segments of three characteristic cross-sections of the structure as shown in Fig. 1. In specific, the cross-sections of the tower-base, of the pile at the MSL and of the pile at the mudline were examined. Rainflow counting and the Palmgren-Miner rule were used for the calculation of the 10-minute fatigue damage. The implementation of the rainflow algorithm by Nielsony (2002, 2009) was employed in all cases, while grouping of magnitudes, accounting for unclosed cycles etc. followed established standards (Hayman 2012). Damage was assessed locally, at the level of the weld itself, rather than at the level of the entire section, using localized stresses rather than force and moment resultants. This enables the determination of crack initiation at specific segments of the cross-section and the consideration of different weld details according to structural steel codes, e.g., Eurocode 3 (CEN 2002).

Two different classes of detail, namely 40 MPa and 71 MPa, were assumed for the welded connection. A detail of 40 MPa corresponds to fillet welds, while a detail of 71 MPa corresponds to butt welds for connecting a circular hollow section to a ring-shaped flange plate. The corresponding S-N curves of Eurocode 3 part 1.9 were employed. For normal stresses, the Wöhler coefficients, representing the log-slope of S-N curves, are equal to m=3 and m=5, the latter applying to lower stress ranges as shown in Fig. 4.

In total, 10 potential values of 10-min fatigue damage were estimated for each of the selected wind speeds. These were used to fit a lognormal distribution at each different mean wind speed. For intermediate values of wind speed where no data was available, linear interpolation was for determining the corresponding parameters of the (lognormal) fatigue damage distribution. The final step was to estimate the annual damage based on the 10-minute damage and the distribution of the annual wind speed data by employing a Monte Carlo simulation. Thus, different samples of 10 min wind speeds were simulated for the period of one year (52596 values in each). Once the annual damage is calculated, the estimated fatigue life in years is equal to its reciprocal. In the present investigation, the turbine is assumed to have 100% availability, while discrete events (startup/shutdown) have been discounted. Despite lacking some code-mandated features in its implementation, the adopted approach comes with a significant advantage compared to conventional approaches encoded in software such as MLife (Hayman 2012): Sources of uncertainty may be efficiently introduced and propagated through the calculation. The aforementioned process of calculating the annual damage (and the corresponding fatigue life) can be repeated numerous times since the distributions of the fatigue damage and the anemological data of the site are known. In this study, 100 such evaluations of the fatigue life were performed, for each of the three cross-sections of interest, offering a useful image of the accuracy achieved even with a limited-scope analysis.

ANALYSIS RESULTS

Case 1: North Aegean Sea

The first site that was examined is in the north part of the Aegean Sea. The distribution of wind speed at 10m (U_{10}) of the MSL in a typical year is shown in Fig. 5. The mean value of wind speed was 5.41 m/s and the standard deviation 2.92 m/s. Interestingly, it was found that for the specific site, the distribution of the wind speed is best modeled by a lognormal distribution and not by the usual Weibull assumption that is

the general case for wind speed. The two options are compared in Fig. 6, where it is shown that both options are relatively accurate for the case at hand. Still, the lognormal can better capture the tails of the distribution in a quantile-quantile plot. Regarding the wind direction, North-East (24.6%) and North (12.9%) constitute the preferred directions in a typical year. Finally, as for the site geography, Table 1 shows the values of fetch for each of the eight main directions considered in this study.

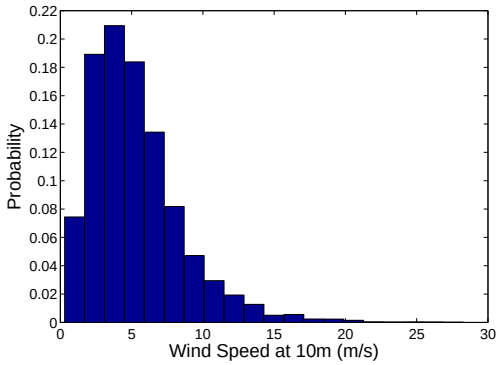

Fig. 5. Distribution of 10-minute non-zero wind speed at 10 m height (North site). There is also a ~30% probability of zero wind occurrence.

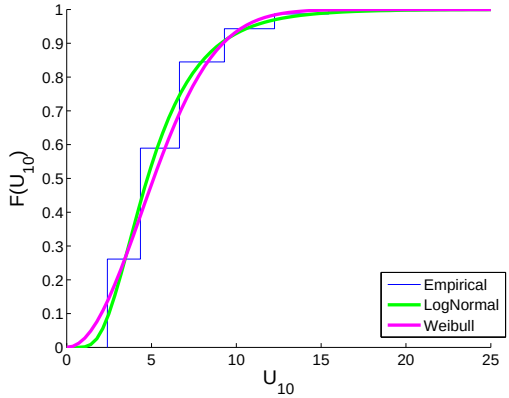

Fig. 6. Cumulative distribution function plot (CDF) of the empirical distribution of wind speed data as compared with Lognormal and Weibull assumptions.

Due to the characteristic lack of actual joint measurements for wind and wave, the next step in the analysis was to estimate the joint PDF $f(H_s,U_{10})$ of wind speed and significant wave height:

$$f(H_s, U_{10}) = f_{H_s/U_{10}}(H_s|U_{10}) f_{U_{10}}(U_{10}) \quad (4)$$

where: $f_{U10}(U_{10})$ is the PDF of U_{10}, which is assumed to follow a lognormal distribution, as mentioned above and $f_{Hs|U10}(H_s|U_{10})$ is the conditional PDF of significant wave height H_s given the wind speed U_{10}. The distribution of the conditional PDF during a given storm is assumed to follow a Rayleigh distribution according to IEC 61400-3. Using Eq. 4, the joint probability between wind speed and significant wave height can be estimated for each wind direction (and corresponding fetch) and the associated probability plots can be constructed. Fig. 7 shows a contour plot of the joint PDF for the North site for all directions combined. The part of the contours forming a characteristic ridge of higher H_s values corresponds to S/SW, where the fetch is higher according to Table 1.

Table 1. Fetch for each of the directions considered (North site).

Direction	Fetch (km)
N	5.8
NE	6.0
E	8.8
SE	34.4
S	73.1
SW	113.6
W	86.2
NW	18.9

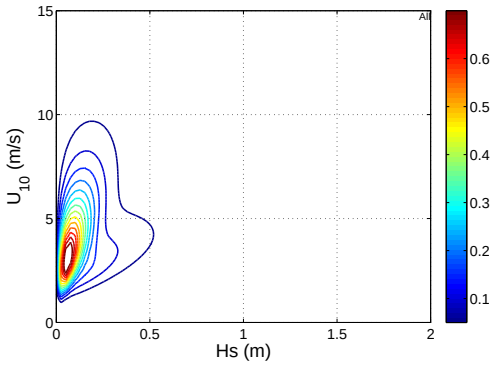

Fig. 7. Contour plot of the joint PDF $f(H_s,U_{10})$ (North site).

Table 2. Wind speed and wave characteristics at the North site.

U_{90} (m/s)	U_{10} (m/s)	T_p (s)	H_s (m)	Dominant Direction	Fetch (km)
3	2.21	1.26	0.08	NE	6.0
5	3.68	1.50	0.12	NE	6.0
10	7.35	1.93	0.20	NE	6.0
15	11.03	2.24	0.30	NE	6.0
20	14.70	2.48	0.40	N	5.8
25	18.38	2.70	0.48	N	5.8
30	22.06	2.90	0.52	N	5.8

From the above PDF, one can determine the directions with the higher contribution for different wind speed values. The direction with the highest contribution for wind speed values up to 15 m/s at hub height (U_{90}) was the North-East (NE), while the North (N) direction dominated speed values larger than 15 m/s. As shown in Table 1. the aforementioned directions are associated with small fetch values of about 5.8 – 6.0 km, thus are associated with low wave heights. The results are shown in Table 2.

A power-law wind profile (IEC 61400-3) was assumed for the distribution of the value of wind speed along the height z. According to this, if the wind speed is known at specific height z_0, the wind speed at height z is given by the formula:

$$U(z) = U(z_0)\left(\frac{z}{z_0}\right)^{\alpha} \quad (5)$$

where α is the power-law exponent, taken to be equal to 0.14, as proposed by IEC 61400-3 for normal wind conditions. For the case at hand, z_0 = 10 m (reference value) and z = 90 m (hub height).

The values of wind speed at hub height and the corresponding wave

characteristics constitute the input to FAST, where the coupled dynamic analysis was performed. At the end of each simulation, time-series of stress history were obtained (e.g., Fig. 8).

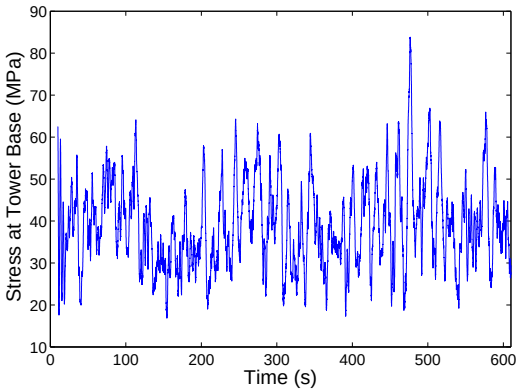

Fig. 8. Typical form of stress time-series.

Fig. 9 shows the histograms of annual fatigue damage and fatigue life at the tower base (D = 6 m, t = 27 mm) from the Monte Carlo simulation. The top plots of Fig. 9 correspond to the 40 MPa detail, while the bottom plots to the 71 MPa butt welds. According to the results of the Monte Carlo analysis, the average annual fatigue damage for a detail of 40 MPa is equal to 0.0124 (with a standard deviation of 0.0011) and the estimated fatigue life is 81.48 years (with a standard deviation of 7.53 years). On the other hand, if a detail of 71 MPa is considered, the average annual fatigue damage is equal to 4.29×10^{-4} (with a standard deviation of 5.51×10^{-5}) and the estimated fatigue life is 2370 years (with a standard deviation of 312.91 years). The huge difference in the estimated life and the huge value in the case of detail 71 MPa is certainly attributed to the nearly 80% higher fatigue resistance that is associated with the better (but also more expensive) detail (EC3, part 1.9).

For the cross-section at MSL (D = 6 m, t = 60mm), non-negligible fatigue damage was observed only for a detail of 40 MPa. The annual fatigue damage and the estimated fatigue life were calculated in the same manner as in the case of tower base. However, a very low value of fatigue damage was observed. In specific, the average annual fatigue damage equals 3.45×10^{-5} (a standard deviation of 3.69×10^{-5}) and thus a huge fatigue life is expected (2933 years with a standard deviation of 313.71 years). This finding is mainly attributed to the larger thickness of the cross-section (t = 60mm versus t = 27mm). As in the case of the cross-section at MSL, non-trivial fatigue damage could be estimated for the cross-section of at the mudline only when a detail of 40 MPa was considered. In specific, the average annual fatigue damage was found to be equal to 0.0038 (with a standard deviation of 3.35×10^{-4}) and the corresponding fatigue life equal to 267.09 years (with a standard deviation of 24.56 years).

Based on the results listed above, a significant conclusion is that the tower base is more vulnerable to fatigue than the other two cross-sections. This finding is easily attributed to the smaller thickness of the cross-section. Furthermore, the detail of weld connection is a crucial factor with a major contribution to fatigue. Finally, given that fatigue is expected to be the governing design situation for the Aegean (where extreme wind-wave loads are generally of limited magnitude), significant economies of scale can be achieved by choosing simpler (and less expensive) weld details, and perhaps even thinner tower cross-sections.

Case 2: South Aegean Sea

The second site of this study was selected to be in the South Aegean. It was also assumed that this site is far enough from shore in order to use the same fetch (equal to 120 km) regardless of direction. This assumption is of course oversimplified but it has the advantage that it does not require the consideration of wind direction in the analysis. At this point, the authors would like to mention a legal limitation that may arise. As of today, Greece has not declared an Exclusive Economic Zone and its territorial waters are extended up to 6 nautical miles from the shore. Thus, any planned offshore wind farm would have to be placed inside the above 6-mile zone. For this reason, a site with such a large omnidirectional fetch may not yet be available for exploitation in the Aegean Sea. However, the analysis was performed in order to evaluate the effect of a duration-limited (rather than fetch-limited) sea state. When the regional politics will allow it, such a case can become more of a practical, rather than a theoretical possibility.

Fig. 10 shows the distribution of the wind speed at 10 m at the South site. A statistical analysis showed that the mean value of the 10-minute wind speed is equal to 7.74 m/s and the standard deviation is equal to 5.10 m/s. Thus, a first inference is that South site is characterized by higher wind speeds than the North site. Finally, it was found that a Weibull (and not a lognormal) distribution with parameters $\lambda = 8.65$ and $k = 1.58$ provides the best fit.

The same assumptions and analysis process as in the case of the North site were undertaken for the estimation of the fatigue damage. Table 3 shows the wind speed and wave characteristics that were used for the dynamic analysis. From Table 3 it becomes obvious that, as expected, the wave intensity characteristics are quite more significant compared to those of the North site. Of course this can be attributed to the longer fetch distances that were employed. Fig. 11 shows the contour plot of the joint PDF $f(H_s,U_{10})$ for the South site, combining all directions. Now, all contours have an “oval” shape since the same fetch is assumed for all directions. In the North site, only South and South-East winds are practically fetch-unlimited, but generally less frequent, this leading to the lower-right lobe appearing in Fig. 7 that is absent from Fig. 11.

The Monte Carlo analysis for a detail of 40 MPa, estimates the average annual fatigue damage at the cross-sections of the tower base to be equal to 0.0407 (with a standard deviation of 0.0036). This value corresponds to an estimated fatigue life of 24.77 years (with a standard deviation of 2.17 years). On the other hand, for a detail of 71 MPa, the average annual damage was equal to 0.0021 (with a standard deviation of 2.43×10^{-4}) and the estimated fatigue life was equal to 494.38 years (with a standard deviation of 59.90 years). The higher values of fatigue damage (and the shorter fatigue lives) for the South site are obviously be attributed to the higher wind and wave characteristics that are associated with the South site. As in the case of the case of the North site, non-negligible fatigue damage of the cross-section at MSL was observed only for a detail of 40 MPa. The average annual fatigue damage was equal to 0.0014 (with a standard deviation of 1.42×10^{-4}) and the estimated fatigue life was equal to 746.58 years (with a standard deviation of 78.66 years). Higher fatigue damage and shorter fatigue life were calculated for the case of the cross-section at mudline in comparison with the North site. In specific, for the detail of 40 MPa, the average annual fatigue damage was equal to 0.0232 (with a standard deviation of 0.0022) and the estimated fatigue life was equal to 43.58 years (with a standard deviation of 4.24 years). For a detail of 71 MPa, fatigue damage was observable but very low. In specific, the average annual fatigue damage was equal to 3.27×10^{-4} (with a standard deviation of 5.30×10^{-5}) and the estimated fatigue life was equal to 3148.60 years (with a standard deviation of 543.46 years).

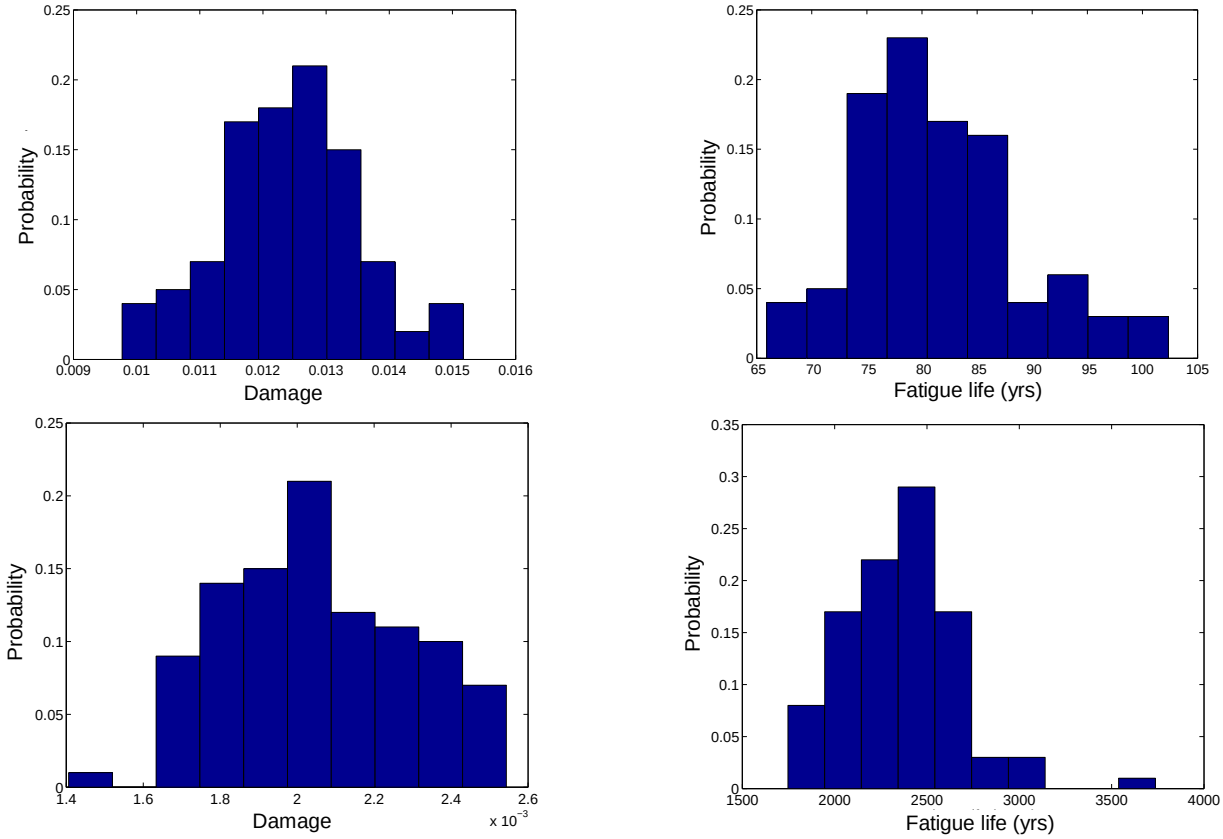

Fig. 9. Probability histograms of fatigue damage (left) and fatigue life (right) at the tower base for weld details rated at 40 MPa (top) and 71 MPa (bottom)

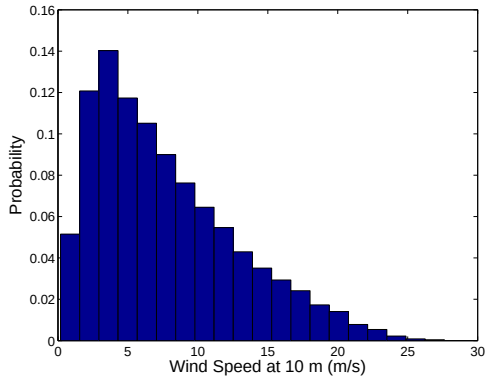

Fig. 10. Distribution of Wind Speed at 10 m height (South site). The zero-wind probability is practically zero.

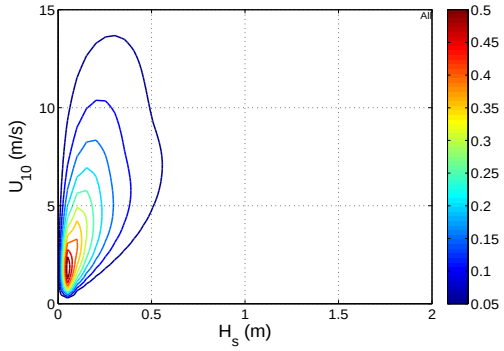

Fig. 11. Contour plot of the joint PDF $f(H_s,U_{10})$ at the South site.

Table 3. Wind speed and wave characteristics at the South site

U_{90} (m/s)	U_{10} (m/s)	T_p (s)	H_s (m)	Fetch (km)
3	2.21	3.42	0.36	120
5	3.68	4.08	0.59	120
10	7.35	5.23	1.24	120
15	11.03	6.08	1.94	120
20	14.70	6.78	2.70	120
25	18.38	7.40	3.50	120
30	22.06	7.96	4.36	120

Based on the results of both sites, it is inferred that for site with higher wind and waves (South site) considerably higher fatigue damage is expected. Furthermore, for both sites, the connection at the tower-base was found to be more vulnerable to fatigue, as a combination of a large lever-arm relative to the hub and a small thickness of its cross-section compared to the pile foundation. The latter, at least in this design, tends to experience larger moments but significantly lower stresses. Similarly, the cross-section at mudline is more vulnerable than the cross-section at MSL: Higher moments are expected to act the mudline, while both cross-sections of this cylindrical pile are the same. Finally, as expected, the lower-quality fillet welds are more vulnerable to

fatigue than butt welds. Still, they are much cheaper to execute, and thus a potential cost-reduction technique for sites with less intensive wind loads. This is expected to be a significant advantage for sites in the Aegean, where the environmental loads are generally more benign compared to the European north.

CONCLUSIONS

A probabilistic fatigue life assessment for a standard offshore wind turbine with a monopile design was presented. Two potential sites of construction in the Aegean Sea of Greece with different wind and wave characteristics were examined. A fully coupled dynamic analysis for the calculation of loadings due to wind and wave was performed using the freely available FAST software. The assessment of fatigue damage (and corresponding fatigue life) for three specific cross-sections of the structure was made considering two different details of welded connections according to Eurocode 3.

The results follow the obvious trends: Turbines at windier sites with longer fetch distances are obviously more vulnerable to fatigue. Lower quality fillet welds similarly attract higher fatigue damage compared to more expensive butt welds. Still, it seems that the wind-wave conditions encountered within a region of the moderate dimensions of the Aegean may vary enough to warrant significantly differentiating the tower design. The detailed view of the effect of uncertainty offered by a detailed probabilistic approach can help in properly quantifying the actual performance of the structural components and thus result to a better compromise between safety and economy. Incorporating further sources of uncertainty (corrosion, detail fatigue strength) and operational states of the wind turbine (e.g., starting and stopping) will only improve the accuracy in such predictions and help offer a cost-effective custom-made solution for a site of interest.

ACKNOWLEDGEMENTS

This research has been co-financed by the European Union (European Social Fund - ESF) and Hellenic national funds through the Operational Program "Competitiveness and Entrepreneurship" of the National Strategic Reference Framework (NSRF 2007-2013) - Research Funding Program: Bilateral R&D Cooperation between Greece and China 2012-2014.

REFERENCES

Arwade, S.R., Lackner, M.A., and Grigoriu, M.D(2011). “Probabilistic Models for Wind Turbine and Wind Farm Performance,” *J Solar Energy Engineering*, ASME, 133, 041006-1-041006-9.

ASTM E1049-85 (1997). “Standard Practices for Cycle Counting in Fatigue Analysis,” *Annual Book of ASTM Standards*, 03.01, 710-718.

DNV-RP-C205(2010). "Environmental Conditions and Environmental Loads," *Det Norske Veritas*, Bærum, Norway.

CEN (2002). “Eurocode 3: Design of Steel Structures, Part 1.9: Fatigue Strength of Steel Strutcures,” *CEN Central Secretariat*, Brussels, Belgium.

IEC 61400-3 (2009). "Wind Turbines-Part 3: Design Requirements for Offshore Wind Turbines," *European Committee for Electrotechinal Standardization*, Brussels, Belgium.

Haselbach, P.U., Natarajan, A., Jiwinangun, R.G., and Branner, K. (2013). “Comparison of coupled and uncoupled load simulations on a jacket support structure.” *Energy Procedia*, 35:244–252.

Hayman, G.J. (2012). “MLife theory manual for version 1.00”, *National Renewable Energy Laboratory*, Golden, CO.

Jonkman, J.D. (2009). “Dynamics of Offshore Floating Wind Turbines – Model Development and Verification,” *Wind Energy*, 12, 459-492

Jonkman, J.D., Butterfield, S., Musial, W., and Scott, G. (2009). “Definition of a 5-MW Reference Wind Turbine for Offshore System Development,” *Tech Report NREL/TP-500-38060*, Golden, CO.

Jonkman, J.D., and Buhl, M.L., Jr. (2005). “FAST User’s Guide,” *Tech Report NREL/EL-500-38230*, Golden, Colorado

Jonkman, B.J., and Kilcher, L. (2012). “TurbSim User’s Guide: Version 1.06.00,” *Tech Report NREL/EL-xxx-xxx (Draft Version)*, Golden, CO.

Kooijman, H.J.T., Lindenburg, C., Winkelaar, D., and van der Hooft, E.L. (2003). “DOWEC 6 MW Pre-Design” *Tech Report DOWEC-F1W2-HJK-01-046/9 (Public Version)*, Petten, Holland

MedPAN(2013). “Overview of Planned OWF Projects in the Mediterranean,” Network of Marine Protected Area Managers in the Mediterranean, Marseille, France.

Moan, T. (2014). “Stochastic Dynamic Response Analysis of Offshore Wind Turbines in a Reliability Perspective,” *Proc. 9th Int Conf Structural Dynamics EURODYN 2014*, Porto, Portugal.

Morison, J., O’Brien, M.P.., Johnson, J.W., and Schaaf, S.A.(1950). “The Force Exerted by Surface Waves on Piles,” *Petroleum Transactions*, 189, 149-154.

Nielsony, A. (2009). “Determination of Fragments of Multiaxial Service Loading Strongly Influencing the Fatigue of Machine Components,” *Mechanical Systems and Signal Processing*, 23(8), 2712-27121.

Nielsony, A. (2002). “Rainflow Counting Method, set of functions with user guide for use with MATLAB”, http://www.mathworks.com/matlabcentral/fileexchange/3026S.

Passon, P., and Branner, K. (2014). "Condensation of Long-Term wave Climates for the Fatigue Design of Hydrodynamically Sensitive Offshore Wind Turbine Support Structures ," *Ships and Offshore Structures*, Taylor & Francis, 1-25.

Sorensen, J.D. (2014). “Reliability Analysis of Wind Turbines Exposed to Dynamic Loads,” P*roc. 9th Int Conf Structural Dynamics EURODYN 2014*, Porto, Portugal.